




Cite this: *Polym. Chem.*, 2025, **16**, 3344

Received 10th April 2025,  
Accepted 8th June 2025

DOI: 10.1039/d5py00359h

rsc.li/polymers

## Oxidation of polydithioacetals towards enhanced interchain interactions and oxidative stability†

Jingman Xie,<sup>a</sup> Kangle Yan,<sup>a</sup> Hailong Wang,<sup>b</sup> Shuo Geng,<sup>a</sup> Yan Gao,<sup>a</sup> Wangmao Tian,<sup>a</sup> Chengcheng Hu<sup>a</sup> and Liang Yuan \*<sup>a</sup>

Polydithioacetals can be readily prepared, while the weak interchain interactions limit their potential applications. Here, controlled oxidation of polydithioacetals to incorporate sulfoxides and sulfones into the main chain was achieved at room temperature by using 3-chloroperoxybenzoic acid (*m*CPBA). The polymer chains maintained good integrity during the oxidation, while the glass transition temperature of the resulting polymers significantly increased from  $-35$  °C to  $110$  °C when all the sulfide groups were oxidized to sulfones. The impact of oxidation on the surface hydrophilicity, thermal stability, mechanical strength and oxidative stability of the polymer was further studied. Overall, the current work provides a new perspective for fine-tuning the chemical structure and properties of polydithioacetals.

### Introduction

Polymers containing dithioacetal groups have recently attracted increasing attention for applications as stimuli-responsive biological materials and covalent adaptable networks.<sup>1–4</sup> Versatile methods are reported to be effective in creating polydithioacetal polymers (PTAs), including acid-catalyzed thiol-aldehyde polycondensation, organic base-promoted thiol-Michael addition between electron-deficient alkynes with polymercaptans, chlorodimethylsilane-assisted reductive etherification of aldehydes with dithiols, ring-opening polymerization of dithioacetal-containing monomers, and thiol-acetal exchange reactions.<sup>5–11</sup> Recently, we have revealed the mechanism of catalyst-free photo-polycondensation between aldehydes and polymercaptans.<sup>12</sup> Aside from applications in nanomaterials or hydrogels, utilization of dithioacetal-containing polymers as bulk materials shows advantages as high refractive index materials, recyclable polymers, and degradable materials.<sup>13–16</sup> However, most linearly structured PTAs exhibit low glass transition temperatures ( $T_g$ s) and limited mechanical performance (Scheme 1A).

Methods to enhance the mechanical properties of PTAs can be categorized into three groups (Scheme 1B): rigid monomers,<sup>14</sup> crosslinking<sup>17–19</sup> and nanocomposites.<sup>20</sup> For example,

a PTA from acid-catalyzed polymerization between 1,6-hexanedithiol and benzaldehyde has a  $T_g$  of  $-29$  °C and is a sticky material (Scheme 1A).<sup>12</sup> When benzaldehyde is copolymerized with a rigid aromatic dithiol, the product shows a  $T_g$  of  $64$  °C and can be used as a high-refractive-index plastic (Scheme 1B).<sup>14</sup> Recently, Zhang has reported the crosslinking of benzaldehyde with a tetra-thiol monomer and obtained recyclable and self-healable networks with a mechanical strength of  $\sim 50$  MPa.<sup>21</sup> Our group reported the interfacial polymerization of 1,6-hexanedithiol and benzaldehyde in a Pickering emulsion stabilized by cellulose nanocrystals, which contain sulfonate groups on the surface to promote condensation reactions.<sup>20</sup> Composite materials with mechanical strengths of up to  $30$  MPa were obtained. Overall, these methods depend on the utilization of unique monomers, while the availability of polymercaptans and aldehyde monomers is relatively limited. Meanwhile, the creation of composite materials complicated the process. A versatile and facile method for tuning the bulk properties of PTAs is highly anticipated.

Here, we report the impact of oxidation by *m*CPBA on the thermomechanical performance, degradability, and surface properties of PTAs, using a linear polymer from the polycondensation between benzaldehyde and 1,6-hexanedithiol as a model (Scheme 1D).<sup>22,23</sup> Although the oxidative degradation of PTAs by reactive oxygen species and by refluxing in DMSO is well documented, no study has been carried out for a milder and controlled oxidation procedure.<sup>5,10,24</sup> The degree of PTA oxidation can be easily tuned by the charging ratio of *m*CPBA to sulfur atoms. As observed, the PTA main chain stays stable while the sulfur atoms are gradually oxidized to sulfoxides and sulfones. With a higher degree of oxidation, the  $T_g$  of the

<sup>a</sup>Anhui Provincial Engineering Center for High Performance Biobased Nylons, School of Materials and Chemistry, Anhui Agricultural University, Hefei, Anhui, 230036, P. R. China. E-mail: yuanliang2020@ahau.edu.cn

<sup>b</sup>Hangmo New Materials Group C. Ltd, Anji, Zhejiang, 313300, China

† Electronic supplementary information (ESI) available: Additional information for digital photos, <sup>1</sup>H NMR, GPC, FT-IR, and XPS results. See DOI: <https://doi.org/10.1039/d5py00359h>



**Scheme 1** (A) Polydithioacetals from the polycondensation between benzaldehyde and 1,6-hexanedithiol, (B) strategies to enhance the mechanical properties of benzaldehyde-based polydithioacetals, and (C) oxidation of sulfides to enhance interchain interactions.

polymer gradually increased to 112 °C, and films can be obtained through hot-pressing. Oxidation will transform the sticky polymer into flexible films and brittle materials due to the sulfone–sulfone interactions between the oxidized chains.<sup>25–27</sup> Interestingly, when the dithioacetal groups are completely converted to sulfones, the product shows good thermal stability and oxidative stability in refluxing DMSO. Thus, the current work provides an alternative perspective for fine-tuning the properties of PTAs.

## Results and discussion

### Oxidation of polydithioacetals

Benzaldehyde is a sustainable raw material, which can be obtained by the chemical conversion of cinnamaldehyde, a key component of plant essential oils.<sup>28</sup> As shown in Scheme 1, it undergoes polycondensation with 1,6-hexanedithiol at room temperature to obtain the polydithioacetal polymer P0 as a transparent viscous product, consistent with our previous report (Fig. S1†). <sup>1</sup>H NMR spectra show a characteristic peak for the dithioacetal proton (–S–CH–S–) at 4.8 ppm (Fig. 1a). Among many oxidants, *m*CPBA was selected due to its high selectivity, mild reaction conditions and ease of control. P0



**Fig. 1** (a) <sup>1</sup>H NMR analysis in d<sub>6</sub>-DMSO, (b) <sup>13</sup>C NMR analysis in d<sub>6</sub>-DMSO, (c) FT-IR spectrum and (d) GPC analysis of P0, P0-0.6 & P0-2.

was then oxidized by *m*CPBA at increasing molar ratios to sulfur atoms (0.4, 0.6, 1.0, and 2.0). The resulting materials were named P0-0.4, P0-0.6, P0-1 and P0-2, respectively.

The oxidized products were analyzed by <sup>1</sup>H NMR (Fig. 1a and Fig. S2†). P0-0.4 and P0-0.6 show apparent splitting and broadening of the protons adjacent to the sulfur atoms (–CH<sub>2</sub>–S–CH–S–CH<sub>2</sub>–) at 4.8 ppm and 2.3 ppm, meaning that a certain ratio of the sulfur atoms was oxidized to sulfoxides. When treated with more *m*CPBA, a complete shift of these protons to 6.8 ppm and 3.2 ppm was observed in P0-2, indicating the conversion of sulfur atoms to sulfones (Fig. 1a). <sup>13</sup>C NMR analysis of P0, P0-0.6 and P0-2 confirmed the same trend (Fig. 1b). The carbon signal near the sulfide group appeared in the region of 25–35 ppm for P0. After oxidation, the signal intensity at the original position of 25–35 ppm decreased significantly, while a new peak appeared in the region of 40–60 ppm, corresponding to carbons near the sulfoxide and sulfone groups.

Oxidation of P0 was further tracked through FT-IR analysis (Fig. 1c and Fig. S3†). After oxidation, a new absorption peak appeared at 1028 cm<sup>–1</sup>, corresponding to the stretching vibration of sulfoxide (S=O) from P0-0.4 and P0-0.6. After increasing the ratio of *m*CPBA, a new absorption peak was observed at 1105 cm<sup>–1</sup> in the spectra of P0-1 and P0-2, corresponding to the stretching vibration of sulfone (O=S=O).<sup>29–31</sup> Thus, on the main chain of P0-1, both sulfoxides and sulfones are present, while it is difficult to quantify their ratios from NMR and FT-IR results. Generally, with a higher *m*CPBA charging ratio, more sulfone groups will be generated.<sup>32,33</sup>

GPC results showed that the number average molecular weight (*M<sub>n</sub>*) of P0 was 13.6 kDa, and the polydispersity index (*D*) was 1.8 (Fig. 1d). To verify the polymer chain integrity after the oxidation process, the oxidized polymer products (P0-0.4, P0-0.6, P0-1, and P0-2) were subjected to GPC analysis (Fig. 1d and Fig. S4†). The *M<sub>n</sub>* of these polymers were found to be 20.8 kDa, 15.7 kDa, 8.1 kDa and 31.2 kDa, respectively, with PDI between 1.8 and 2.3. P0-1 showed a decreased molecular

weight as compared to P0, and the reason was still unknown after repeating the experiment and analysis. Thus, during the oxidation, the polymer chains maintained good integrity without major chain breakage.

With the transformation of sulfur atoms into sulfoxides or sulfones, the surface properties of P0 will be altered. All polymers were comparatively analyzed by X-ray photoelectron spectroscopy (XPS), as shown in Fig. 2a–c and Fig. S5.† In the sulfur element analysis diagram, the P0 S 2p spectrum shows two peaks, corresponding to S 2p<sub>3/2</sub> (binding energy ≈ 163 eV) and S 2p<sub>1/2</sub> (≈164 eV) of sulfide (–S–), and the oxidation state of sulfur is –2. With moderate oxidation as shown in P0-0.6, the characteristic peak of sulfoxide (S=O, S + 4) appears (S 2p<sub>3/2</sub> ≈ 165 eV, S 2p<sub>1/2</sub> ≈ 166 eV), while the sulfide peak intensity was decreased and sulfoxide accounted for about 50%–70%. With the highest degree of oxidation (P0-2), the sulfone peak dominates (S + 6 accounts for more than 90%), the residue of sulfoxide is less than 5%, and the sulfide disappears completely (Fig. 2c).<sup>34–37</sup>

The water contact angle is a key index to measure the wettability of a material's surface, which reflects the polarity characteristics and hydrophilicity of the material's surface. The introduction of sulfoxide (S=O) or sulfone (O=S=O) may have an influence on its surface polarity and wettability.<sup>31,38,39</sup> The water contact angle test results for P0 before and after oxidation are shown in Fig. 2d. The water contact angle of P0 was 84.7°, which indicated obvious hydrophobicity. With increasing degrees of oxidation, the water contact angle of the product firstly decreased gradually to 51.5° for polymer P0-1, indicating that its surface wettability was significantly improved and its hydrophilicity was enhanced with more sulfoxide groups on the main chain. Interestingly, P0-2, which has a high degree of sulfonation, shows a similar water contact angle (84.8°) to that of P0. This phenomenon arises because both sulfoxide and sulfone moieties can engage in hydrogen

bonding with water; however, the hydrogen bonds formed by sulfoxide groups are significantly stronger than those formed by sulfone groups, which is well documented.<sup>40,41</sup> Meanwhile, the sulfone–sulfone bonding is reported to be a strong interaction, further forbidding its interaction with water.<sup>25</sup>

### Thermal and mechanical properties

Sulfoxides and sulfones are polar functionalities compared to sulfides. Sulfone–sulfone non-covalent interactions were found to contribute to the polymer's mechanical properties (Fig. 3a). Recently, salt-responsive polymer assemblies were obtained through a polymerization-induced sulfone-bond-driven self-assembly process.<sup>26</sup> In the current work, by treating with increasing ratios of *m*CPBA, the resulting polymer would contain more polar moieties (sulfoxide or sulfone). According to DSC analysis (Fig. 3b), P0 has a glass transition temperature (*T*<sub>g</sub>) of –35.7 °C. After oxidation, the *T*<sub>g</sub>s of the resulting materials were found to be –19.0 °C, 69.0 °C, 79.8 °C and 110.2 °C for P0-0.4, P0-0.6, P0-1 and P0-2, respectively. Apparently, *T*<sub>g</sub> of P0 can be facily manipulated by *m*CPBA oxidation. The impact of oxidation on the polymer thermal stability is then evaluated by TGA (Fig. 3c). From the discussion above, we know that P0-2 is almost completely oxidized and all the sulfur atoms are converted to sulfones, while the other polymers (P0-0.4, P0-0.6, and P0-1) have different ratios of sulfide, sulfoxide, and sulfone. The initial decomposition temperature (D5, the temperature at which the polymer loses 5% of its original weight) of P0 is calculated to be 283.5 °C, indicating good thermal stability. With increasing degrees of oxidation to P0-0.4, P0-0.6 and P0-1, the thermal stability was apparently sacrificed. These three polymers started to degrade at temperatures below 170 °C. In contrast, the fully oxidized polymer P0-2 shows a D5 of 293 °C and a much higher residue percentage at 700 °C (~20%) than P0 (~5%), indicating enhanced thermal stability. The presence of sulfoxide will



Fig. 2 XPS analysis of polymers (a) P0, (b) P0-0.6, and (c) P0-2; (d) water contact angles of P0 and the oxidized polymer products.

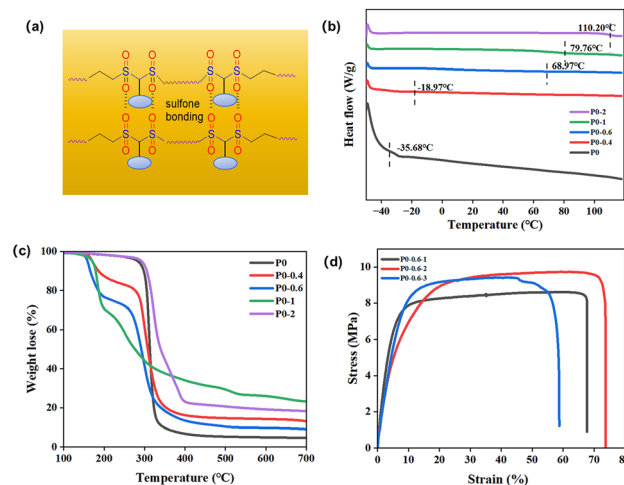


Fig. 3 (a) Schematic illustration of sulfone–sulfone interactions between the oxidized polydithioacetal polymers; (b) DSC and (c) TGA analyses of P0 and the oxidized polymer products; and (d) tensile test results of polymers P0-0.6.

reduce the thermal stability of the sulfide polymers, while sulfone groups will increase their thermal stability.<sup>31,42</sup> As extensively documented in the prior literature, sulfoxide groups within the polymer backbone are susceptible to the Pummerer rearrangement reaction upon heating. This intramolecular rearrangement involving the SO group disrupts the polymer structure, facilitating premature thermal degradation and thereby lowering the decomposition temperature of poly-sulfoxides.<sup>42</sup> In contrast, the sulfone ( $-\text{SO}_2-$ ) groups present in polysulfones lack this specific rearrangement pathway. Their higher oxidation state and symmetrical structure confer greater thermal robustness.<sup>43</sup>

Polymer P0 is a highly tacky and viscous polymer and not suitable for mechanical testing. After the oxidation, all polymers (except P0-0.4) show apparently enhanced hardness over P0. Through a hot-pressing step, free-standing plastic films can be obtained from the oxidized products (Fig. S1†). We noticed that both polymers P0-1 and P0-2 were too brittle for carrying out tensile testing. In contrast, polymers P0-0.6 are flexible films and show a stress-at-break of over 8 MPa and a strain-at-break of >60%. Thus, with the optimized degree of oxidation, the mechanical properties of P0 can be easily tuned, while the mechanism lies in the molecular chain interactions within the oxidized products.

### Degradation studies

Poly(dithioacetal) polymers undergo oxidative degradation,<sup>10</sup> catalytic photodegradation<sup>18</sup> and cation-triggered degradation.<sup>12</sup> The degradability offers merits for their post-usage treatment. Choosing P0-0.6 and P0-2 as examples, we evaluated their oxidative degradation performance by refluxing in DMSO.

P0-0.6 was easily degraded into low molecular weight products (Fig. 4). After refluxing in DMSO for 36 hours, the initial colorless solution turned to a dark colored solution (Fig. 4a). When the degradation study was carried out in  $d_6$ -DMSO,  $^1\text{H}$  NMR analysis of the products indicated the disappearance of the peak at 4.5–5.0 ppm, which corresponds to the proton on the carbon of the initial dithioacetal group. Meanwhile, the proton for the aldehyde group appeared around 9.8 ppm, indicating the regeneration of benzaldehyde (Fig. 4b). The observation is similar to our previous report on the degradation of a vanillin-based polydithioacetal polymer due to a Swern oxidation mechanism.<sup>10</sup> GPC analysis of the resulting solution shows no peak for high-molecular-weight products (Fig. 4c).

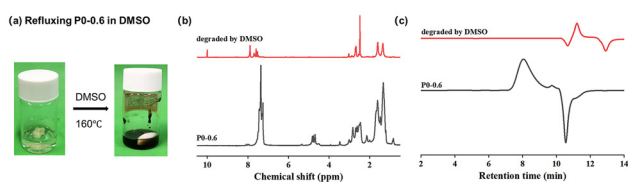


**Fig. 4** (a) Photographs showing the treatment of P0-0.6 in DMSO; (b)  $^1\text{H}$  NMR and (c) GPC analyses of P0-0.6 before and after DMSO oxidation.

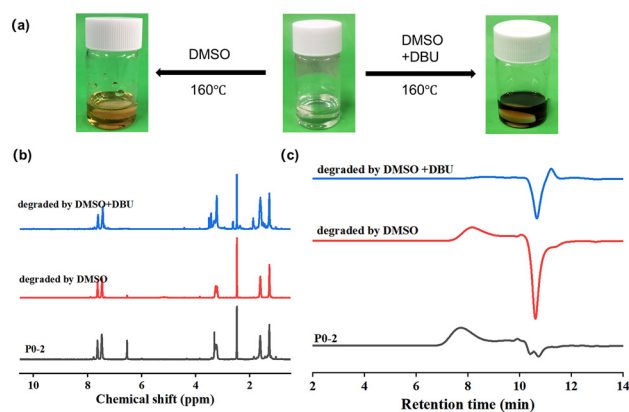


**Fig. 5** (a) Photographs showing the treatment of P0-2 in DMSO and DMSO-DBU; (b)  $^1\text{H}$  NMR and (c) GPC analyses of P0-2 before and after the degradation study.

When polymer P0-2 was treated similarly, no significant degradation was observed, and the solution maintained good clarity (Fig. 5a).  $^1\text{H}$  NMR analysis indicates the presence of almost all the characteristic peaks of P0-2, while no aldehyde peak was detected (Fig. 5b). However, the acetal proton at 6.8 ppm largely disappeared. We attribute this observation to the H-D exchange between P0-2 and  $d_6$ -DMSO at high temperature, due to the acidity of the acetal proton, which is connected to two strong electron-withdrawing sulfone groups. As a controlled study,  $\text{CF}_3\text{COOH}$  is added to the P0-2 solution in  $d_6$ -DMSO, and the acetal proton can still be detected after heating for 36 hours (Fig. S6†). GPC analysis of the treated polymer also shows similar elution curves to that of the untreated product (Fig. 5c). Thus, the complete sulfonation process by *m*CPBA enhanced their oxidative stability under DMSO treatment.

Alternatively, when an organic base (DBU) was added into the solution at a 5% weight ratio of P0-2, the sulfone-containing polymer could be easily degraded at 160 °C as confirmed by  $^1\text{H}$  NMR and GPC testing. After decreasing the temperature to 130 °C, the acetal proton was still observed after heating in  $d_6$ -DMSO-DBU for 36 hours. Thus, a high temperature is necessary to promote the degradation of P0-2 in DMSO-DBU solution (Fig. S7†). The acidity of the protons on the carbons adjacent to the sulfone groups ( $-\text{CH}_2-\text{SOO}-\text{CHPh}-\text{SOO}-\text{CH}_2-$ ) might shed light on the degradation mechanism of P0-2 under basic conditions, as demonstrated in previous studies on the degradation of sulfone-containing polymers.<sup>44,45</sup>

## Experimental

### Materials

1,6-Hexanedithiol (99%), dimethyl sulfoxide (DMSO, 99.94%), and sodium bicarbonate ( $\text{NaHCO}_3$ , 99.5%) were purchased from Bidepharm. Sodium bisulfite was purchased from Macklin, and benzaldehyde (99%), 3-chloroperoxybenzoic acid (*m*CPBA, 75%), and ammonia (AR, 25–28%) were purchased

from Aladdin. Trifluoroacetic acid ( $\text{CF}_3\text{COOH}$ , 99%) was purchased from Energy Chemical, and dimethylformamide (DMF) and anhydrous ether (AR) were purchased from ZhanYun. DBU and dichloromethane (DCM, AR) are from General Agents. All chemicals were used as received without further purification.

### Instruments

A 600 MHz Agilent DD2 branch magnetic resonance spectrometer (Agilent Technology Company of the United States) was used to record the  $^1\text{H}$  NMR and  $^{13}\text{C}$  NMR spectra, and  $d_6$ -DMSO was used for all tests. Fourier-transform infrared spectroscopy (FT-IR, Bruker of Germany) was performed using a Tensor II Fourier transform infrared spectrometer. The spectra were obtained *via* attenuated total reflection (ATR) technology. The test scanning range is  $400\text{--}4000\text{ cm}^{-1}$ , the resolution is  $4\text{ cm}^{-1}$ , and the scanning speed is  $0.2\text{ cm s}^{-1}$ . Gel permeation chromatography (GPC) (Agilent Technology Company of Germany) with a G1316A detector, an Agilent 1260 HPLC pump and PL gel (MIXED-A, effective molecular weight range 200–2 000 000) was used to determine the molecular weight and molecular weight distribution of the polymer samples. The samples were dissolved in *N,N*-dimethylformamide at  $2\text{ mg ml}^{-1}$  and filtered with a filter with an aperture of  $0.22\text{ }\mu\text{m}$  before measurement. A Netzsch 200F3 DSC (TA of the United States) was used to check the glass transition temperature ( $T_g$ ) of the polymer samples. First, the sample was heated from room temperature to  $120\text{ }^\circ\text{C}$  at  $10\text{ }^\circ\text{C min}^{-1}$  and kept at equilibrium for 3 min to remove the heat history. Then, the temperature was immediately dropped to  $-4\text{ }^\circ\text{C}$  for 3 min before being gradually increased to  $12\text{ }^\circ\text{C}$  at  $1\text{ }^\circ\text{C min}^{-1}$ . The thermal stability of the films was measured by thermogravimetric analysis (TGA instrument, Netzsch 209F3, TA of the United States) at a heating rate of  $10\text{ }^\circ\text{C min}^{-1}$  from room temperature to  $100\text{ }^\circ\text{C}$  and maintained for 10 min. Then they were heated to  $600\text{ }^\circ\text{C}$  at  $10\text{ }^\circ\text{C min}^{-1}$  under a nitrogen atmosphere ( $80\text{ mL min}^{-1}$  flow rate). About 8 mg is used for each sample. X-ray photoelectron spectroscopy (XPS, Thermo Fisher Scientific K-Alpha of the United States) spectra were recorded using KRATOS, AXIS SUPRA+, and the profiles were analyzed using the XPSPEAK software system. The tensile test (Shenzhen Sansi Company of China) was carried out on the UTM250 2 universal testing machine equipped with a 500 N sensor at room temperature. The tensile sample was prepared into a standard bone-like spline with a cutting knife and tested at the speed of  $5\text{ mm min}^{-1}$ . Static water contact angles were measured by using the sessile droplet method with a dosing volume of  $2.0\text{ }\mu\text{l}$  and a dosing rate of  $1.0\text{ }\mu\text{l s}^{-1}$ . The result was acquired by taking the average value from more than ten measurements.

### Oxidation of polymer P0

The polydithioacetal polymer P0 was prepared from 1,6-hexanedithiol and benzaldehyde according to our previous report.<sup>10</sup> Then, P0 was oxidized by *m*-CPBA with different molar ratios (0.4, 0.6, 1.0, 2.0) of *m*-CPBA to the sulfur atoms in P0, and the resulting polymers are named P0-0.4, P0-0.6, P0-1,

and P0-2. The oxidation process is the same and the preparation of P0-0.4 is given here for demonstration. At room temperature, polymer P0 (3 g, 0.0252 mol S) was dissolved in 40 ml of DMF in a round-bottom flask. 3-Chloroperoxybenzoic acid (2.157 g, 0.0937 mol) was completely dissolved in 5 ml of DMF and then added to the above round bottom flask. The mixture was stirred at room temperature for 12 hours before adding 50 ml of saturated sodium bisulfite solution dropwise, and the mixture was stirred for 2 hours. The precipitated polymer was washed with 100 ml of saturated sodium bicarbonate for 2 hours and then rinsed with anhydrous ether three times. The product was finally dried in a vacuum oven at  $70\text{ }^\circ\text{C}$  to have P0-0.4.

### Degradation study of the oxidized polymers

The degradation of the oxidized polymers was evaluated by refluxing in DMSO- $d_6$ . Briefly, 100 mg of the polymer is dissolved in 5 ml of DMSO- $d_6$  and refluxed at  $160\text{ }^\circ\text{C}$  for 36 hours in an oil bath. Photographs of the solution are taken before and after the reaction. The solution is utilized for GPC and  $^1\text{H}$  NMR tests for molecular weight and structural information. For polymer P0-2, another degradation test was carried out by adding 5 mg of DBU to the polymer solution (0.1 g in 5 ml DMSO- $d_6$ ) and heating at  $160\text{ }^\circ\text{C}$  for 36 hours before GPC and  $^1\text{H}$  NMR analyses.

## Conclusions

In summary, we carried out a systematic study on the impact of oxidation on the properties of polydithioacetals. By controlling the ratio of *m*-CPBA to the sulfur atoms, the degree of conversion to sulfoxides and sulfones can be tuned, which has a direct impact on the wetting, thermal, mechanical and degradation performances of the resulting polymers. In particular, the  $T_g$  of the initial polymer was increased from  $-35\text{ }^\circ\text{C}$  to  $110\text{ }^\circ\text{C}$  after the complete transformation of sulfides to sulfones. Meanwhile, the polymer turned from tacky to be elastic and brittle with an increased degree of oxidation. The partially oxidized product maintained oxidative degradation capability in refluxing DMSO, while the completely oxidized product was stable after a similar treatment but could be degraded by an organic base. Overall, the current work provides a new perspective for tuning the properties of polydithioacetals besides the monomer structures and forming nanocomposites.

## Author contributions

Jingman Xie: data curation, investigation, project administration, and writing – original draft; Kangle Yan: data curation and investigation; Hailong Wang: funding acquisition and writing – review & editing; Shuo Geng, Yan Gao, Wangmao Tian and Chengcheng Hu: investigation, project administration, and validation; Liang Yuan: funding acquisition, supervision, and writing – review & editing.

## Data availability

The data supporting this article have been included as part of the ESI.†

## Conflicts of interest

There are no conflicts to declare.

## Acknowledgements

The authors acknowledge the funding support from the National Natural Science Foundation of China (52373096), the Natural Science Foundation of Anhui Province (2208085MC69), and Anhui Agricultural University.

## References

- E. Akar, U. Tunca and H. Durmaz, *Eur. Polym. J.*, 2024, **221**, 113532.
- Y. Gu, S. Li, Y. Yu, J. Zhu, X. Yuan, X. Feng and Y. Lu, *Macromol. Rapid Commun.*, 2024, **45**, 2300631.
- A. C. Renner, S. S. Thorat and M. P. Sibi, *RSC Sustainability*, 2024, **2**, 3669–3703.
- Y. Gu, R. Jia, Y. Yu, S. Li, J. Zhu, X. Feng and Y. Lu, *ACS Appl. Mater. Interfaces*, 2024, **16**, 10805–10812.
- S. Kim, H. Park, F. Fuß and Y. Lee, *Polym. Chem.*, 2023, **14**, 2610–2616.
- S. Du, S. Yang, B. Wang, P. Li, J. Zhu and S. Ma, *Angew. Chem., Int. Ed.*, 2024, **63**, e202405653.
- S. Chatterjee and S. Ramakrishnan, *ACS Macro Lett.*, 2012, **1**, 593–598.
- S. Luleburgaz, E. Akar, U. Tunca and H. Durmaz, *Polym. Chem.*, 2024, **15**, 371–383.
- N. Van Herck, D. Maes, K. Unal, M. Guerre, J. M. Winne and F. E. Du Prez, *Angew. Chem., Int. Ed.*, 2020, **59**, 3609–3617.
- Y. Jin, C. Hu, J. Wang, Y. Ding, J. Shi, Z. Wang, S. Xu and L. Yuan, *Angew. Chem., Int. Ed.*, 2023, **62**, e202305677.
- J.-X. Lei, Q.-Y. Wang, F.-S. Du and Z.-C. Li, *Chin. J. Polym. Sci.*, 2021, **39**, 1146–1154.
- W. Tian, J. Wang, Y. Jin, Y. Cheng, K. Yan, C. Hu, C. Chen, B. Wang, Z. Wang and L. Yuan, *Angew. Chem., Int. Ed.*, 2025, e202421231.
- A. O. Kassim, L. S. Kariyawasam and Y. Yang, *Macromolecules*, 2025, **58**, 3395–3406.
- S. Watanabe, T. Yano, Z. An and K. Oyaizu, *ChemSusChem*, 2025, **18**, e202401609.
- L. S. Kariyawasam, J. F. Highmoore and Y. Yang, *Angew. Chem., Int. Ed.*, 2023, **62**, e202303039.
- E. Vasiliev, A. Bukhtoyarova, V. Shelkovnikov, V. Berezhnaya and I. Shundrina, *Polym. Eng. Sci.*, 2025, **65**, 1448–1461.
- R. Li, C. Hu, Y. Lu, W. Tian, T. Tang, Y. Jin, K. Yan, Y. Yan, B. Wang and L. Yuan, *ACS Appl. Polym. Mater.*, 2024, **6**, 11529–11537.
- C. Hu, Y. Jin, W. Tian, K. Yan, J. Wang and L. Yuan, *Macromolecules*, 2024, **57**, 1725–1733.
- Y. Jin, W. Tian, Y. Cheng, C. Hu, J. Wang, B. Wang and L. Yuan, *Macromolecules*, 2024, **57**, 7439–7448.
- Y. Cheng, J. Xie, Y. Lu, W. Tian, T. Wu, F. Chen, W. Gao, Y. Jin, L. Yuan and B. Wang, *ACS Macro Lett.*, 2024, **13**, 1605–1611.
- C. Cui, X. Zhao, X. Wang, Y. Guo, K. Chen, J. Ma, X. Yan, Y. Cheng, Z. Ge and Y. Zhang, *Polym. Chem.*, 2025, **16**, 1595–1602.
- R. Kakarla, R. G. Dulina, N. T. Hatzenbuehler, Y. W. Hui and M. J. Sofia, *J. Org. Chem.*, 1996, **61**, 8347–8349.
- V. V. González and J. Podlech, *Eur. J. Org. Chem.*, 2021, 5430–5442.
- B. Liu and S. Thayumanavan, *Cell Rep. Phys. Sci.*, 2020, **1**, 100271.
- F. Du, B. Qiao, T. D. Nguyen, M. P. Vincent, S. Bobbala, S. Yi, C. Lescott, V. P. Dravid, M. O. Cruz and E. A. Scott, *Nat. Commun.*, 2020, **11**, 4896.
- J. Zhang, Q. Li, T. Yu, Y. Ma, Z. Zhao, C. Shen, X. Liu and M. Huo, *Macromolecules*, 2025, **58**, 1621–1629.
- Y. Zhang, F. Wang, L. Pan, B. Wang and Y. Li, *Macromolecules*, 2020, **53**, 5177–5187.
- X. Luo, Z. Ma, T. Su, X. Xie, Z. Qin, H. Ji and J. Chen, *ChemistrySelect*, 2024, **9**, e202401475.
- Z. Zhao, X. Chen, Q. Wang, T. Yang, Y. Zhang and W. Z. Yuan, *Polym. Chem.*, 2019, **10**, 3639–3646.
- X. Cai, X. Zhao, S. Mahmud, X. Zhang, X. Wang, J. Wang and J. Zhu, *Biomacromolecules*, 2024, **25**, 1825–1837.
- Z. Beyazkiliç, G. Lligadas, J. C. Ronda, M. Galià and V. Cádiz, *Polymer*, 2015, **68**, 101–110.
- S. Choi, J.-D. Yang, M. Ji, H. Choi, M. Kee, K.-H. Ahn, S.-H. Byeon, W. Baik and S. Koo, *J. Org. Chem.*, 2001, **66**, 8192–8198.
- S. Koo, K. Ahn, S. Byeon, J. Yang, M. Ji and S. Choi, *WIPO*, WO0162719, 2001.
- M. Podgórski, C. Wang, Y. Yuan, D. Konetski, I. Smalyukh and C. N. Bowman, *Chem. Mater.*, 2016, **28**, 5102–5109.
- G. Zhang, S.-s. Yuan, Z.-m. Li, S.-r. Long and J. Yang, *RSC Adv.*, 2014, **4**, 23191–23201.
- Z. Wu, D. Li, Z. Wei, X. Wang, S. Long, J. Yang and G. Zhang, *ACS Appl. Mater. Interfaces*, 2023, **15**, 19527–19535.
- Y. Deng, R. Wang, Z. Ma, W. Zuo and M. Zhu, *J. Agric. Food Chem.*, 2023, **71**, 18857–18864.
- L. I. Teixeira, K. Landfester and H. Therien-Aubin, *Macromolecules*, 2021, **54**, 3659–3667.
- E. Fulajtar and S. Agarwal, *ACS Appl. Polym. Mater.*, 2024, **6**, 10768–10778.
- G. Perell, R. Staebell, M. Hairani, A. Cembran and W. C. K. Pomerantz, *ChemBioChem*, 2017, **18**, 1836.
- L. Teixeira, K. Landfester and H. Thérien-Aubin, *Macromolecules*, 2021, **54**, 3659–3667.

- 42 J. M. Sarapas and G. N. Tew, *Macromolecules*, 2016, **49**, 1154–1162.
- 43 D. Kaiser, I. Klose, R. Oost, J. Neuhaus and N. Maulide, *Chem. Rev.*, 2019, **119**, 8701–8780.
- 44 C. M. P. Casey and J. S. Moore, *ACS Macro Lett.*, 2016, **5**, 1257–1260.
- 45 T. Shinoda, T. Nishiwaki and H. Inoue, *J. Polym. Sci., Part A: Polym. Chem.*, 2000, **38**, 2760–2766.